Length scales in turbulent free shear flows

Length scales in turbulent free shear flows

G. Cafiero[a] and M. Obligado[b] and J.C. Vassilicos[c]

[a] Department of Mechanical Engineering Sciences, University of Surrey, Guildford, GU2 7HX, UK
[b] Univ. Grenoble Alpes, CNRS, Grenoble INP, LEGI, 38000 Grenoble, France
[c] Univ. Lille, CNRS, ONERA, Arts et Métiers ParisTech, Centrale Lille, FRE 2017 - LMFL - Laboratoire de Mécanique des fluides de Lille - Kampé de Feriet, F-59000 Lille, France

ARTICLE HISTORY
Compiled March 22, 2020

ABSTRACT
In the present paper, we address the important point of the proportionality between the longitudinal integral lengthscale (L) and the characteristic mean flow width (δ) using experimental data of an axisymmetric wake and a turbulent planar jet. This is a fundamental hypothesis when deriving the self-similar scaling laws in free shear flows, irrespective of turbulence dissipation scaling. We show that L/δ is indeed constant, at least in a range of streamwise distances between 15 and 50 times the characteristic inlet dimension L_{ref} (nozzle width or wake generator size). Furthermore, we revisit turbulence closure models such as the Prandtl mixing length [1] and the constant eddy viscosity in the light of the recent non-equilibrium dissipation scalings. We show that the mixing length model, with $l_m \sim \delta$, does not comply with the scalings stemming from the non-equilibrium version of the theory even if it does comply with the theory's equilibrium version; we instead obtain $l_m \sim \delta\sqrt{Re_G/Re_{0\delta}}$, where Re_G and $Re_{0\delta}$ are a global and local Reynolds number, respectively for the recent non-equilibrium dissipation scalings. Similarly, the eddy viscosity model holds in the case of the non-equilibrium version of the theory provided that the eddy viscosity is constant everywhere, not only across sections orthogonal to the streamwise direction as in the equilibrium case. We conclude by comparing the results of the different models with each other and with experimental data and with an improved model (following Townsend) that corrects for the eddy viscosity by taking into account the intermittency of the flow.

KEYWORDS
Jets; Wakes; Non equilibrium turbulence; Turbulence modeling.

1. Introduction

Free shear flows are of significant importance in many natural and industrial applications. They are also of great interest for fundamental research, as it is one of the few cases in turbulence where mean quantities can be predicted under a small, physically based, set of hypotheses. The theory, developed by Townsend [2] and later by George [3], requires the self-preservation of some turbulence quantities in the mean momentum and streamwise kinetic energy equations. In order to close the equations, an *ad*

Email: g.cafiero@surrey.ac.uk
Email: martin.obligado@univ-grenoble-alpes.fr
Email: john-christos.vassilicos@centralelille.fr

hoc assumption is required to model the dissipation term in the kinetic energy equation. The closure usually chosen is the one consistent with the Richardson-Kolmogorov cascade, in which case one assumes that the centreline turbulence dissipation rate ε can be described as $\varepsilon = C_\varepsilon K^{3/2}/L$, where K is the turbulent kinetic energy, L is an integral length-scale of the turbulence (usually taken to be the longitudinal one) and C_ε is a dimensionless coefficient which may depend on boundary conditions but is independent of Reynolds number at high enough Reynolds number values. Finally, the integral lengthscale L is assumed to be proportional to a mean flow profile width such as the wake/jet width δ.

Focusing on the free shear flows investigated in the present work, namely the axisymmetric wake and the planar jet, this theoretical approach leads to the following streamwise evolutions of the centreline velocity (jet) or velocity deficit (wake) u_0 and the jet or wake width δ:

$$u_0 \sim (x - x_0)^a, \tag{1}$$

$$\delta \sim (x - x_0)^b, \tag{2}$$

with $a = -1/2$ and $b = 1$ for the planar jet and $a = -2/3$ and $b = 1/3$ for the axisymmetric wake [2], [3], [4] (x is the streamwise coordinate and x_0 is a virtual origin).

Previous to Townsend [2] and George [3], researchers were already able to predict these exact same streamwise dependencies of δ and u_0 under different assumptions. A closure of the mean momentum equation can be given by assuming that the relevant component of the Reynolds shear stress tensor, $\overline{u'v'}$, is related to the streamwise mean flow velocity $\overline{u}$ by

$$\overline{u'v'} = -\nu_T \frac{\partial \overline{u}}{\partial y} \tag{3}$$

where y is the spreading direction of the flow and ν_T is the eddy viscosity; here and in the following, the overline symbol indicates ensemble averaging. The modelling of ν_T has been the focus of intense research during the first half of the 20th century ([5], [6], [7], [8]) and has been studied for many free shear flows. The most basic and common hypotheses used are Prandtl's mixing length hypothesis,

$$\nu_T = l_m^2 \left| \frac{\partial \overline{u}}{\partial y} \right|, \tag{4}$$

where l_m is the mixing length, and a constant eddy viscosity hypothesis

$$\nu_T = L_{eddy} U_{eddy} \tag{5}$$

where L_{eddy} and U_{eddy} are characteristic scales of length and velocity, respectively, which may depend on x but are constant along y.

Equations 1 and 2 are retrieved with $l_m \sim \delta$ and $L_{eddy} \sim \delta$. In this sense, the Richardson-Kolmogorov cascade (which is one of the pillars of the Townsend-George approach given that it adopts $\varepsilon \sim K^{3/2}/\delta$) is consistent with both the constant eddy viscosity and Prandtl's mixing length hypotheses.

	Equilibrium	Non-equilibrium
Dissipation Scaling	$K_0^{3/2}/\delta$	$(Re_G/Re_\delta)K_0^{3/2}/\delta$
Power laws exponents: Axisymmetric Wake	$a=-2/3$, $b=1/3$	$a=-1$, $b=1/2$
Power laws exponents: Planar Jet	$a=-1/2$, $b=1$	$a=-1/3$, $b=2/3$

Table 1. Summary of the dissipation, mean flow (u_0) and characteristic flow width (δ) scalings obtained according to the equilibrium and the non-equilibrium versions of the Townsend-George theory for the axisymmetric wake and turbulent planar jet cases.

	Equilibrium	Non-equilibrium	Label
Mixing Length	$l_m \sim \delta$	$l_m \sim \delta\sqrt{Re_G/Re_{0\delta}}$	M1
Eddy Viscosity	$\nu_T \sim u_0\delta$	$\nu_T \sim U_{ref}L_{ref}$	M2
Corrected eddy viscosity	$\nu_T \sim \gamma u_0\delta$	$\nu_T \sim \gamma U_{ref}L_{ref}$	M3

Table 2. Summary of the mixing length (l_m) and eddy viscosity (ν_T) scalings obtained according to the equilibrium and the non-equilibrium versions of the Townsend-George theory for the axisymmetric wake and turbulent planar jet cases. The last column indicates the label used for the plots later in the paper.

Recent works have unveiled the presence of turbulence dissipation scalings in grid-generated turbulence, periodic turbulence and free shear flows which are at odds with the Richardson-Kolmogorov scaling for ε ([9], [10], [11], [12], [13]). Direct numerical simulations (DNS) and experiments for axisymmetric wakes and experimental data for the plane jet suggest the presence in free shear flows of the new non-equilibrium scalings for dissipation, at least for a large portion of the flow. The dissipation parameter C_ε is no longer independent of Reynolds number (though it does remain independent of the fluid's kinematic viscosity ν), but scales as Re_G/Re_δ where $Re_G = U_{ref}L_{ref}/\nu$ is the global Reynolds number (U_{ref} is the free stream or inlet velocity and L_{ref} is a characteristic inlet lengthscale such as the wake generator's size or the nozzle width) and $Re_\delta = \sqrt{K_0}\delta/\nu$ is a local Reynolds number (K_0 is the turbulent kinetic energy on the flow centreline). As shown by Dairay et al [10] and Cafiero and Vassilicos [9], the application of the non-equilibrium dissipation scaling makes it possible to use a smaller number of assumptions than Townsend [2] and George [3] and leads to new exponents for eq. (1) and (2). In the planar jet case, $a=-1/3$ and $b=2/3$ while in the axisymmetric wake case, $a=-1$ and $b=1/2$. It is important to explicitly notice that the assumption $L \sim \delta$ is needed for both the classical and the non equilibrium dissipation scalings. In table 1 we summarise the scalings stemming from the Richardson-Kolmogorov equilibrium dissipation and the non-equilibrium dissipation versions of the theory.

One easily checks that the Prandtl mixing length hypothesis cannot lead to (1) and (2) with non-equilibrium exponents if $l_m \sim \delta$. The non-equilibrium scalings can however be retrieved if $l_m \sim \delta\sqrt{Re_G/Re_{0\delta}}$ (see table 2) where $Re_{0\delta} = u_0\delta/\nu$ (see table 1). As for the constant eddy viscosity, it can still be used to obtain non-equilibrium scaling exponents a and b but only if ν_T is constant throughout the flow so that $\nu_T \sim U_{ref}L_{ref}$, not only across sections of the flow orthogonal to the streamwise coordinate as in $\nu_T \sim u_0\delta$.

In this work we first and foremost address one key aspect of the Townsend-George approach using experimental data for a turbulent axisymmetric wake at $Re_G = 40000$ and a planar jet at $Re_G = 20000$: the important question of the proportionality of L and δ in free shear flows. Secondly, we also ask whether the equilibrium and non-equilibrium mixing length and eddy viscosity models imply different mean flow profiles

and how the different models perform in predicting these profiles.

Prandtl's mixing length and the constant eddy viscosity are both very simple closures that have been known for decades. Nevertheless, they remain used in the wider fluid dynamics community for computational fluid dynamics and simple theoretical modelling [14]. We have therefore chosen this simple and well known closures to show the important consequences of non-equilibrium turbulence for modelling. To the best of authors' knowledge, no systematic study of the modelling and applicability of this hypothesis has been done previously for different turbulence dissipation laws. Furthermore, we provide the first theoretical model that gives the mean transverse profiles in terms of the Richardson-Kolmogorov and non-equilibrium cascades. The second part of this manuscript is devoted to showing some simple consequences of the recent non-equilibrium dissipation (and therefore cascade) scalings for turbulence modelling, which might in the future be expanded to more complex and/or more complete models [15].

2. Experimental setup

The experiments were carried out in two different facilities at Imperial College London. A schematic representation of both the planar jet and the axisymmetric wake flows is provided in figure 1.

The planar jet flow is generated using a centrifugal blower which collects air from the environment and then forces it into a plenum chamber. In order to reduce the inflow turbulence intensity level and remove any bias due to the feeding circuit, the air passes through two sets of flow straighteners before entering a convergent duct (having area ratio equal to about 8). At the end of the duct there is a letterbox slit with aspect ratio $w/L_{ref} = 31$ (with $L_{ref} = 15$ mm being the slot width in the y direction). In order to produce a top hat entrance velocity profile, the two longest sides of the slit are filleted with a radius $r = 2L_{ref}$, following the careful recommendation by [16]. The jet exhausts in still ambient air and is confined in the spanwise direction by two perspex walls of size $100L_{ref} \times 100L_{ref}$ placed in $x-y$ planes . The rotational speed of the blower is controlled using an in-house PID controller to produce an inlet Reynolds number $Re_G = 20000$. Single (SW) and Cross (XW) wire measurements are taken along the jet centreline in the range $x/L_{ref} = 14 - 50$ with $2L_{ref}$ spacing. Both SW and XW are driven by a Dantec Streamline constant temperature anemometer (CTA). Data are sampled at a frequency of 50 KHz, with measurements lasting 60 s and 120 s respectively in the SW and XW cases.

The wake flows were generated in the low-turbulence wind tunnel at Imperial College London. The measurement test section is 3 ft x 3 ft (≈91 cm x 91 cm) and length 4.25 m. The plates employed for these experiments have a reference length $L_{ref} = \sqrt{A_{plate}} = 64$ mm, with thickness 1.25 mm, A_{plate} being the frontal area of the plate. The plate is suspended in the centre of the wind tunnel normal to the laminar free stream using four 1 mm diameter piano wires. The free-stream velocity was kept fixed at U_{ref}=10 m/s using a PID controller. For that value, the velocity fluctuations around the mean are below 0.1% when the plate is not in place. The velocity signal is measured using a one component hot-wire (herein referred to as SW) driven by a Dantec Streamline constant temperature anemometer (CTA). Data are sampled at a frequency of 20 KHz . Each measurement lasts for 60 s, which was deemed to be sufficient to converge the integral scales. The choice of U_{ref} is conditioned by the wind tunnel properties: while for lower values the wind tunnel is unstable, for larger values

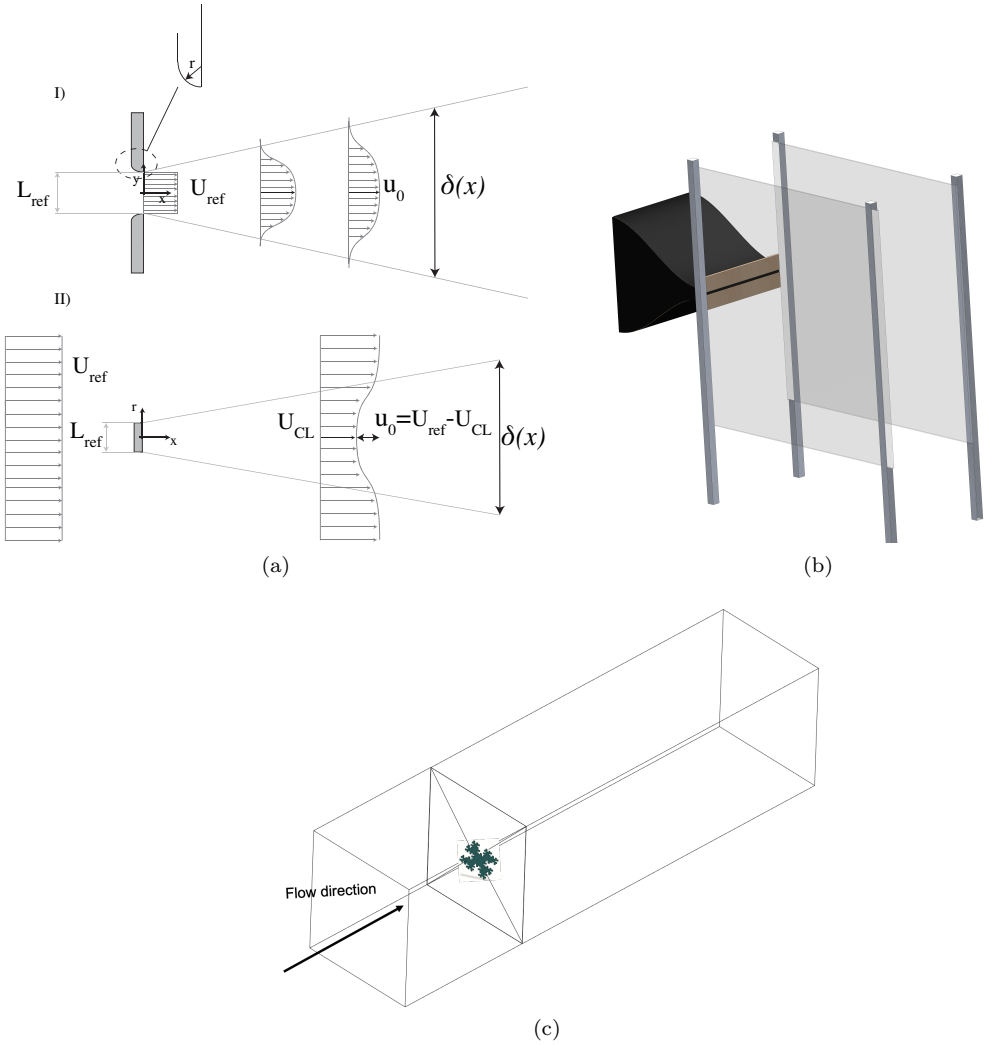

Figure 1. a-I) Schematic representation of the planar jet flow and three dimensional representation of the planar jet facility (b); a-II) Schematic representation of the axisymmetric wake flow. $\delta(x)$ is representative of the characteristic flow width at each streamwise location x which is defined as $\delta(x) = 1/u_0 \int_0^\infty u dy$ and $\delta(x)^2 = 1/u_0 \int_0^\infty (U_{ref} - u) r dr$ in the jet and wake cases, respectively. c) Three dimensional representation of the wake generating body and its positioning within the wind tunnel.

of U_{ref} the air tends to heat, diminishing the reliability of the SW measurements. Finally, a X-wire probe was used to estimate the kinetic energy only for centreline measurements. The centreline kinetic energy is calculated by assuming axial symmetry, i.e. $K_0 = 0.5\left(\overline{u'^2} + 2\overline{u_r'^2}\right)$ where u' and u_r' are streamwise and radial fluctuating velocities obtained by the Reynolds decomposition of the velocity field. More details about the experimental set-up can be found in [10,11].

The longitudinal integral lengthscale L is calculated by converting the anemometer time signal into space using the frozen turbulence hypothesis and using the autocorrelation of the fluctuating streamwise velocity. Comparison of the results with those obtained using the expression in [17], *i.e.* $L = \pi E_u(k = 0)/\overline{u'^2}$ (where E_u is the streamwise velocity power spectral density), shows minimal discrepancies. The estimate of the turbulent dissipation rate ε is obtained from its isotropic surrogate, i.e. $\varepsilon_{ISO} = 15\nu\overline{(\partial u'/\partial x)^2}$, by integrating the one dimensional spectrum of the velocity signal $F_{11}^{(1)}$ as follows

$$\overline{(\partial u'/\partial x)^2} = \int_0^\infty k^2 F_{11}^{(1)} dk. \tag{6}$$

In both the experiments, we took care of reducing the noise at the high wavenumber end of the spectrum. As suggested by [11], we fit the portion of the spectrum at frequencies higher than Kolmogorov's frequency with an exponential law. It must be however pointed out that the contribution of this portion of the spectrum to the integral in equation (6) is always less than 6%.

3. Results

Townsend [2], George [3], Dairay et al [10] and Cafiero & Vassilicos [9] assumed that the dissipation lengthscale $C_\varepsilon K^{3/2}/\varepsilon$ could be interchangeably taken to be proportional to the integral lengthscale L or the characteristic flow width δ without loss of validity of their results, at least in terms of scaling. It is then pertinent to investigate this assumption by looking at data measured for two different wake-generating bodies, a square plate and a fractal-perimeter plate (see [10,11] for more details), as well as for the planar jet. Data are taken along the flows' centreline. The inlet Reynolds numbers are $Re_G = 40000$ and 20000 for the wakes (based on the square root of the plates' area) and jet (based on the nozzle width), respectively.

Figure 2a supports the assumption of proportionality between L and δ, at least in the range of streamwise distances $15 \leq x/L_{ref} \leq 50$ (with departure from a constant value always smaller than $\pm 5\%$), which is part of the region where the non-equilibrium dissipation scaling holds as reported in [9–11]. A constant value of the ratio L/δ is attained both in the wake and the jet cases, but the value of the constant seems to vary from flow to flow. In general, there is no reason to expect any sort of universality for this ratio. For example, the planar jet is characterized by larger entrainment, thus entailing higher spreading rate and flow width δ. Conversely, we do not expect to see any significant effect of the inlet Reynolds number Re_G for a particular flow. As shown in [10], an increase in the global Reynolds number by almost a factor 7 ($Re_G = 5000$ for DNS data and $Re_G = 40000$ in the experiments) lead to unchanged values of the wake width δ. Furthermore, in the turbulent regime the integral lengthscale L does not vary much with Re_G.

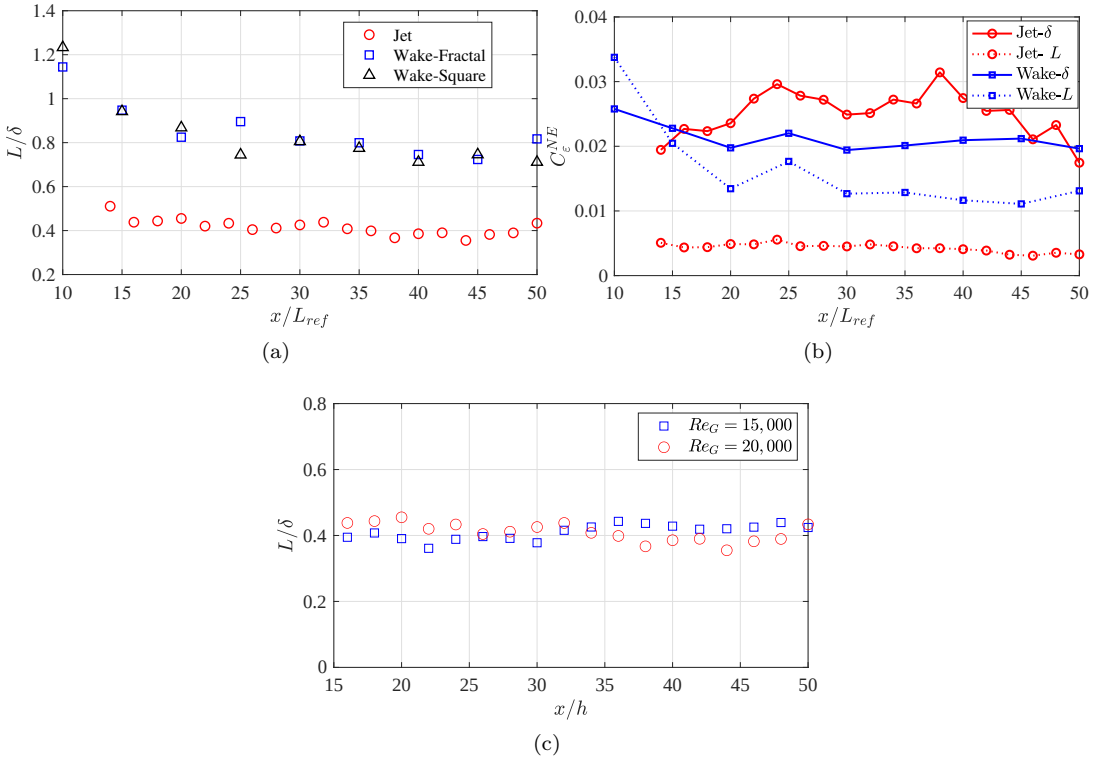

Figure 2. a)Streamwise profiles of L/δ for the planar jet (red circles), the axisymmetric fractal wake (blue squares) and the axisymmetric square wake (black triangles). The ratio is calculated along the centreline of the flow. Inlet Reynolds numbers $Re_G = 40000$ (wakes) and 20000 (jet). b) Non-equilibrium dissipation constant $C_\varepsilon^{NE,\delta} = (U_{ref}L_{ref})^{-1}\varepsilon\delta^2/K_0$ for the the planar jet (red circles-continuous) and the axisymmetric fractal wake (blue squares-continuous). Non-equilibrium dissipation constant $C_\varepsilon^{NE,L} = (U_{ref}L_{ref})^{-1}\varepsilon L^2/K_0$ for the planar jet (red circles-dotted) and the axisymmetric fractal wake (blue squares-dotted). c) Streamwise profiles of L/δ for the planar jet case measured at two different global Reynolds numbers, $Re_G = 20,000$ and $Re_G = 15,000$.

Similar conclusions can be drawn for the planar jet. In this case, it is possible to directly investigate the effect of Re_G on the value of L/δ. Figure 2c shows the streamwise variation of the ratio L/δ measured at $Re_G = 20,000$ and $Re_G = 15,000$.

Figure 2b compares the profiles of C_ε^{NE} (defined in the caption of figure 2) as a function of the streamwise distance when calculated using either L or δ. We plot the data for the turbulent planar jet and the axisymmetric wake of the fractal obstacle only, as the square one exhibits similar trends. Regardless of the choice of L or δ, C_ε^{NE} exhibits the same constant behaviour, as required by the non-equilibrium turbulence dissipation scaling.

3.1. Lateral Profiles

In this section we investigate the consequences of the application of a different turbulence dissipation scaling on the lateral mean flow profiles. The scalings (1) and (2) stemming from the version of the theory based on the recent non-equilibrium dissipation scalings, can also be obtained with the mixing length,

$$l_m \sim \delta\sqrt{Re_G/Re_{0\delta}}, \tag{7}$$

but not with $l_m \sim \delta$ (see table 2).

Similarly, for the constant eddy viscosity model, the version of the theory based on the recent non-equilibrium dissipation scalings returns the right exponent a and b provided that ν_T is not only constant across a section orthogonal to the mean flow as in the equilibrium case, but throughout. Introducing into equation (3) the scalings of $\langle u'v' \rangle$ stemming from the version of the theory with the different non-equilibrium dissipation scalings (see [10] and [9]), we obtain

$$-\nu_T \frac{\partial \overline{u}}{\partial y} = u_0^2 \frac{d\delta}{dx}, \tag{8}$$

for the planar jet case [9] and

$$-\nu_T \frac{\partial \overline{u}}{\partial y} = U_{ref} u_0 \frac{d\delta}{dx}, \tag{9}$$

for the axisymmetric wake case [10], [11]. Introducing the power laws (1) and (2) with the non-equilibrium values of a and b reported in table 1,

$$\nu_T \sim U_{ref} L_{ref} \sim const, \tag{10}$$

both for the planar jet and for the axisymmetric wake case, as opposed to

$$\nu_T \sim u_0 \delta, \tag{11}$$

obtained from the equilibrium version of the Townsend-George theory (which actually requires one more assumption to conclude, see [10] and [9]).

It is then important to determine whether the differences in mixing length and eddy viscosity are reflected in different mean flow profiles for different turbulent dissipation scalings. Furthermore, it is also relevant to determine whether the mean flow profiles

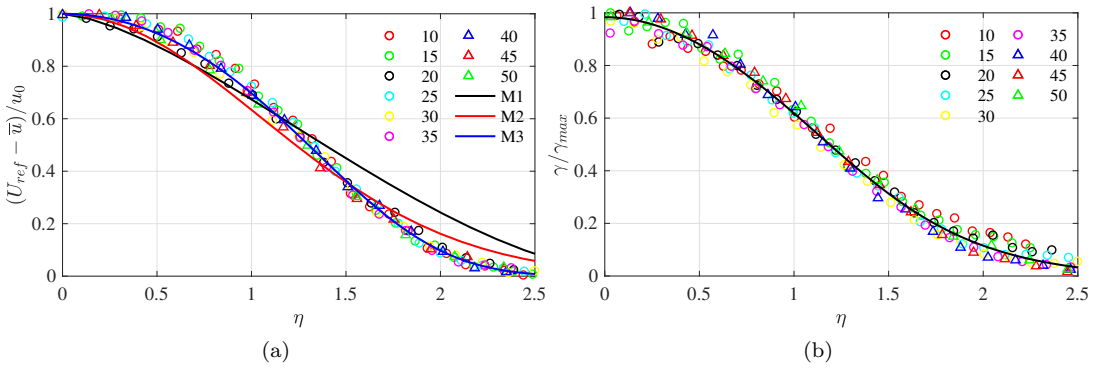

Figure 3. a) Mean flow velocity profiles for the axisymmetric wake in the range of streamwise distances $10 \leq x/L_{ref} \leq 50$ (symbols). Black, red and blue lines are representative of Prandlt mixing length model (M1, eq. 12), eddy viscosity model (M2, eq. 13) and eddy viscosity corrected with the intermittency (M3, eq. 16), respectively. b) Intermittency factor in the range of streamwise distances $10 \leq x/L_{ref} \leq 50$ rescaled with respect to its local maximum. The continuous line is representative of equation 15. Data are plotted against the similarity coordinate η. The inlet Reynolds number is $Re_G = 40000$.

obtained with the Prandtl mixing length or with the constant eddy viscosity models are consistent with the experimental data, and more or less so depending on turbulence dissipation scaling.

Mixing-length based models [6,8] have largely proven to be inadequate for correctly predicting lateral mean flow profiles. By comparing with experimental results obtained in the turbulent planar wake of a square cylinder, Townsend [7] found that a constant eddy viscosity $\nu_T \sim u_0\delta$ best represented his measurements. We also compare the mixing length based model and constant value of the eddy viscosity to each other and to our data, but by taking into account the non-equilibrium modification of these two models. Furthermore, following Townsend's approach [7], we also correct the eddy viscosity to account for the intermittency of the flow. In the following we compare our experimental data with mean flow profiles predicted by Prandtl's mixing length and constant eddy viscosity models for the axisymmetric wake and the planar jet.

The detailed derivations of the profiles stemming from these two models modified to take into account the non-equilibrium dissipation (and therefore cascade) are reported in the appendix.

3.1.1. Axisymmetric Wake

For an axisymmetric wake, when using Prandtl's mixing length (eq. 4) to model the Reynolds shear stress it is possible to show that the mean flow profile can be described as [6] (see Appendix)

$$\frac{U_{ref} - \overline{u}}{u_0} = \sqrt{x} f(\eta) = \left(1 - \left(\frac{\eta}{\eta_0}\right)^{3/2}\right)^2, \tag{12}$$

where $\eta = y/\delta$ and $\eta = \eta_0$ is the point where $f \to 0$ on the boundary of the wake (see Appendix).

When, instead, a constant value of the eddy viscosity is used (eq. 5), the following

form of the mean flow can be obtained [18]:

$$\frac{U_{ref} - \overline{u}}{u_0} = e^{-\frac{k\eta^2}{2}}, \tag{13}$$

with $\eta = y/\delta$; k depends on the turbulence dissipation scaling (see Appendix). It is worth noting that the profiles obtained in equations (12)-(13) are valid for both turbulence dissipation scalings (classical equilibrium and new non-equilibrium).

Figure 3a shows the mean flow velocity profiles rescaled with the maximum at each streamwise location plotted against the similarity variable r/δ. A comparison of the two proposed models (eq. 12-13) suggests that Prandtl's mixing length model overestimates the velocity profile for values of $r/\delta > 1$. A constant value of the eddy viscosity seems to follow more closely the physics of the problem. As also showed by Townsend [7], a significant improvement of the eddy viscosity model can be obtained by accounting for the intermittency factor γ. It is important to state explicitly that, in the present context, the intermittency relates to the interface between vortical and potential flow at the edges of a free shear flow [4]; it is not related to the internal intermittency which is thought to cause the deviations from Kolmogorov theory [19].

The intermittency can be calculated as the inverse of the kurtosis of the time derivative of the streamwise fluctuating velocity, *i.e.*,

$$\gamma = \frac{1}{\mathrm{Kurt}[du'/dt]}. \tag{14}$$

This is due to the fact that the eddy viscosity cannot be non-zero beyond the turbulent/non-turbulent interface, where there are no vortical fluctuations at all. Following Townsend, we use a functional form for the intermittency as

$$\frac{\gamma}{\gamma_{max}} = \frac{1}{\left(1 + (\eta/\alpha_1)^2 + (\eta/\alpha_2)^4 + (\eta/\alpha_3)^6\right)} \tag{15}$$

with α_1, α_2 and α_3 parameters to be determined, (with no significant dependence on the Reynolds number) and we redefine the eddy viscosity as $\nu_T^I = \gamma\nu_T$.

Equation (15) requires that the intermittency factor is self preserving; this is a condition satisfied in our experiments as can be observed from Figure 3b where we plot the intermittency profiles obtained in the range of streamwise distances $10 \leq x/L_{ref} \leq 50$ normalised with respect to the local maximum at each streamwise location. The continuous line is representative of the fit of equation (15) and shows a remarkable agreement with the experimental data.

Hence, we modify the eddy viscosity by accounting for the intermittency of the flow, *i.e.* $\nu_T^I = \nu_T\gamma$, with ν_T a constant value and we find a solution to the self-similar equation of the form

$$\frac{U_{ref} - \overline{u}}{u_0} = e^{-k\eta^2\left(\frac{1}{2} + \frac{1}{4}(\eta/\alpha_1)^2 + \frac{1}{6}(\eta/\alpha_2)^4 + \frac{1}{8}(\eta/\alpha_3)^6\right)}. \tag{16}$$

We seek the coefficients α_1, α_2, α_3 and k which optimise equations 15 and 16 simultaneously. The continuous blue line in figure 3a shows that the introduction of the intermittency factor significantly improves the results, particularly in proximity of the wake boundaries. The choice of this particular form of the intermittency profile makes

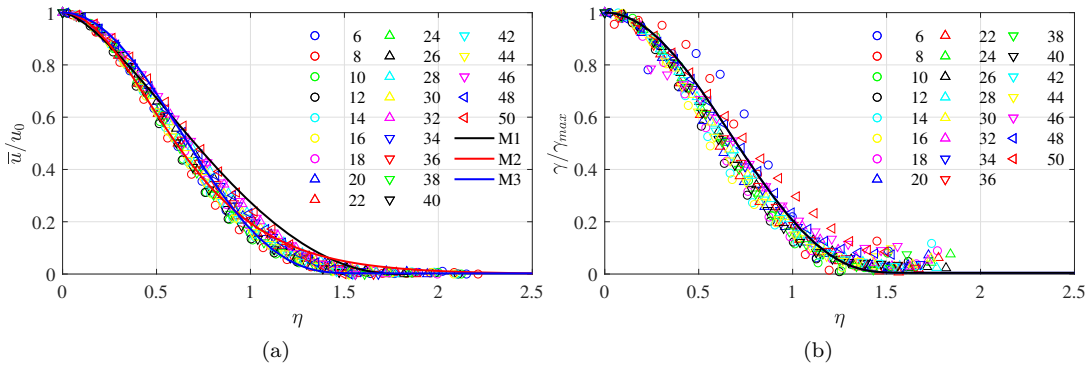

Figure 4. a) Mean flow velocity profiles for the turbulent planar jet in the range of streamwise distances $6 \leq x/L_{ref} \leq 50$ (symbols). Black, red and blue lines are representative of Prandlt mixing length model (M1, numerical solution of eq. 17), eddy viscosity model (M2, eq. 19) and eddy viscosity corrected with the intermittency (M3, numerical solution of eq. 20), respectively. b) Intermittency function rescaled with respect to the local maximum at each streamwise position x/L_{ref} in the range $6 \leq x/L_{ref} \leq 50$. The black line is representative of the fit $\frac{\gamma}{\gamma_{max}} = f(\eta)^m$. Data are plotted against the similarity coordinate η. The inlet Reynolds number is $Re_G = 20000$.

it possible to obtain a closed form of the mean flow profile [7] which complies with the self-preservations of the intermittency and mean flow profiles at once.

3.1.2. Planar Jet

We follow a similar procedure in the planar jet case. The application of Prandtl's mixing length model leads to the following form of the jet momentum equation

$$-kF''^2 + FF' = 0 \tag{17}$$

where $F'(\eta) = f(\eta)$, $f(\eta) = \overline{u}(x,y)/u_0(x)$, and k a constant value which depends on the turbulence dissipation scaling (this dependence is reported in the Appendix). Nevertheless, as for the axisymmetric wake, there is no substantial difference in the functional form of the mean flow profile for the classical equilibrium and new non-equilibrium cases. As reported by Abramovich [20], Tollmien [21] was the first to find a numerical solution for equation (17). We also solve the equation numerically, comparing the results with our experimental measurements and with the results obtained with the eddy viscosity assumption with/without the intermittency correction.

The adoption of the turbulent viscosity model, leads to the following momentum equation in similarity variables

$$FF'' + F'^2 = -kF''' \tag{18}$$

with $k = \frac{2\nu_T}{u_0 \delta \frac{d\delta}{dx}}$. This equation can be solved to obtain the velocity profile $f(\eta)$

$$f(\eta) = sech^2(\eta\sqrt{2k}). \tag{19}$$

In Figure 4a we report the experimental data obtained from the planar jet experiment in the range of streamwise distances $6 \leq x/L_{ref} \leq 50$, along with the mean flow profiles predicted by the Prandtl mixing length model (M1, black) and the eddy viscosity model

(M2, red). Despite only little differences can be detected throughout the whole range of lateral locations, it can be argued that the Prandtl model slightly underestimates the mean flow profile at small values of η and provides an overestimate of the data for $\eta > 0.6$.

Even though the eddy viscosity model shows good agreement with the experimental data, we decided to try and improve it by accounting for the intermittency of the flow, hence introducing $\nu_T^I = \nu_T \gamma$.

As already discussed in the axisymmetric wake case, this requires that the intermittency function is self-similar. In Figure 4b we compare the data obtained in the range $6 \leq x/L_{ref} \leq 50$ rescaled with respect to the local maximum at each streamwise location (γ_{max}). It can be concluded that γ is indeed self-similar. The momentum equation for the turbulent planar jet hence modifies as

$$\left(F'F \right)' = -k\gamma F''', \tag{20}$$

where $F'(\eta) = f(\eta)$. The solution depends on the choice of γ; we introduce a function $\gamma(\eta) = f(\eta)^m$ and we integrate numerically equation (20). The choice of a different intermittency function is mainly driven by the fact that equation (15) does not lead to a closed solution of equation (20), and we therefore consider a better choice by relating the intermittency function directly to the mean flow. This can also be instrumental in future investigations aimed at relating the intermittency function γ to the turbulence cascade. As evidenced in Figure 4a the solution obtained with the introduction of the intermittency function (blue line) gives a slight improvement to the fit of the experimental data.

4. Conclusions

Using experimental data from a turbulent planar jet and two axisymmetric turbulent wakes, we find evidence for the proportionality of the integral lengthscale L and the characteristic flow width δ in the range of streamwise distances $15 \leq x/L_{ref} \leq 50$. This is a fundamental hypothesis when deriving the self-similar scaling laws in turbulent free shear flows, and it is now established in a region where the turbulent dissipation scaling is of the now known new non-equilibrium type.

We then revisit basic turbulence closure models such as Prandtl's mixing length [1] and constant eddy viscosity in the light of the new non-equilibrium dissipation scalings. In this framework, the cornerstone of Prandtl's (1925) model, *i.e.* $l_m \sim \delta$, is not valid. We show that $l_m \sim \delta\sqrt{Re_G/Re_{0\delta}}$ instead. The scalings (1) and (2) stemming from the non-equilibrium cascade agree with the eddy viscosity model $\nu_T \sim U_{ref} L_{ref}$ rather than $\nu_T \sim u_0 \delta$, hence implying a constant value of the eddy viscosity everywhere in the region where the new non-equilibrium turbulence dissipation scaling holds.

However, we also demonstrate that these differences do not lead to different mean flow profiles. A systematic comparison of the mean flow profiles predicted by Prandtl (1925) and the eddy viscosity models with the experimental data for the axisymmetric wake and the turbulent planar jet reveals the inadequacy of Prandtl's mixing length hypothesis to correctly predict the mean flow behaviour even where the turbulence dissipation has a non-equilibrium cascade scaling. Furthermore, following Townsend [7] we show that the prediction can be further improved by accounting for the inter-

mittency of the flow, particularly in the axisymmetric wake case. In agreement with Townsend [7], we find that rescaling the eddy viscosity ν_T with the intermittency function γ provides a better representation of the mean flow behaviour as it accounts for the eddy viscosity drop across the turbulent flow's intermittent boundaries.

Acknowledgements

GC and JCV were supported by ERC Advanced Grant 320560 awarded to JCV.

Appendix A: governing equations

In this Appendix we report about the equations that lead to the definition of the lateral profiles for the axisymmetric wake and the planar jet flows, following [10] and [9] respectively. We start by describing the axisymmetric wake, then particularise the radial profiles according to the different closure models for the Reynolds stresses.

Axisymmetric wake

For this flow the momentum balance can be approximated as,

$$U_{ref}\frac{\partial}{\partial x}(U_{ref}-\overline{u}) = -\frac{1}{r}\frac{\partial}{\partial r}(r\overline{u'v'}). \tag{21}$$

Assuming that $U_{ref}-\overline{u} = u_0 f(\eta)$, and substituting in equation (21)

$$U_{ref}\frac{\partial u_0}{\partial x}(f(\eta)) - U_{ref}u_0 f'(\eta)\eta\frac{1}{\delta}\frac{\partial \delta}{\partial x} = -\frac{1}{r}\frac{\partial}{\partial r}(r\overline{u'v'}). \tag{22}$$

Momentum flux constancy $u_0\delta^2 = U_{ref}\theta^2$ can be differentiated to get

$$\frac{\partial}{\partial x}u_0 = -2\frac{u_0}{\delta}\frac{\partial}{\partial x}\delta, \tag{23}$$

so we rewrite the momentum equation as

$$\frac{2U_{ref}u_0}{\delta}\frac{\partial}{\partial x}(\delta)f(\eta) + U_{ref}u_0 f'(\eta)\eta\frac{1}{\delta}\frac{\partial}{\partial x}\delta = \frac{1}{r}\frac{\partial}{\partial r}(r\overline{u'v'}). \tag{24}$$

The solution of equation (24) depends on the Reynolds stress modelling. As reported by Goldstein [6], the classical streamwise dependent eddy viscosity based on Prandtl's mixing length (Prandtl (1925)),

$$\nu_T = l_m^2\left|\frac{\partial}{\partial r}(U_{ref}-\overline{u})\right|, \tag{25}$$

leads to the following equation,

$$f' = -\sqrt{\left(\frac{\eta f}{k}\right)}, \tag{26}$$

with $k = \frac{l_m^2 u_0}{\delta^2 \delta' U_{ref}}$. This equation has the solution,

$$\frac{U_{ref} - \overline{u}}{u_0} = f(\eta) = \left(1 - \left(\frac{\eta}{\eta_0}\right)^{3/2}\right)^2, \tag{27}$$

where $\eta_0 = (9k)^{1/3}$ is the point at the boundary of the wake (and therefore where $f \to 0$). Now, depending on the properties of the turbulent cascade, two different closures can be obtained:

i) Richardson Kolmogorov cascade:

In this case, we have $l_m = C\delta$, with C a constant. Furthermore, the streamwise scalings are $u_0 = AU_{ref}(\frac{x-x_0}{\theta})^{-2/3}$ and $\delta = B\theta(\frac{x-x_0}{\theta})^{1/3}$. Adding the integral form of momentum conservation ($u_0\delta^2 = U_{ref}\theta^2$), we get that $k = 3\frac{C^2}{B^3}$ and $\eta_0 = 3\frac{C^{2/3}}{B}$.

ii) Non-equilibrium cascade:

In this case, we have $l_m = C\delta\sqrt{Re_G/Re_{0\delta}} = C\sqrt{U_{ref}L_{ref}\frac{\delta}{u_0}}$, and again C is a constant. In this case, the streamwise scalings are $u_0 = AU_{ref}\left(\frac{x-x_0}{L_{ref}}\right)^{-1}(\theta/L_{ref})^2$ and $\delta = B\sqrt{L_{ref}(x-x_0)}$. Therefore, the constant becomes $k = 2\left(\frac{C}{B}\right)^2$ and $\eta_0 = 18^{1/3}\left(\frac{C}{B}\right)^{2/3}$.

Conversely, the adoption of a turbulent eddy viscosity model, $\nu_T = constant$ delivers a substantially different lateral velocity profile

$$\frac{U_{ref} - \overline{u}}{u_0} = e^{-\frac{k\eta^2}{2}}, \tag{28}$$

with $\eta = y/\delta$ and $k = \frac{U_{ref}\delta\frac{d\delta}{dx}}{\nu_T}$. Once more, two different closures can be obtained:

i) Richardson Kolmogorov cascade:

We have $\nu_T = Cu_0\delta$, with C constant, and we find that $k = \frac{1}{3}\frac{B^3}{C}$.

ii) Non-equilibrium cascade:

In this case, we have $\nu_T = CU_{ref}L_{ref}$. The constant becomes $k = \frac{1}{2}\frac{B^2}{C}$.

On the other hand, Townsend [7], studying the planar wake, suggested that the quality of the fit could be further improved by accounting for the intermittency of the flow γ. He proposed the use of γ in a modified eddy viscosity $\nu_T^I = \gamma\nu_T$ where

$$\frac{\gamma}{\gamma_{max}} = \frac{1}{\left(1 + (\eta/\alpha_1)^2 + (\eta/\alpha_2)^4 + (\eta/\alpha_3)^6\right)}, \tag{29}$$

leading to the following correction of equation (28)

$$\frac{U_{ref} - \overline{u}}{u_0} = e^{-k\eta^2\left(\frac{1}{2} + \frac{1}{4}(\eta/\alpha_1)^2 + \frac{1}{6}(\eta/\alpha_2)^4 + \frac{1}{8}(\eta/\alpha_3)^6\right)}, \tag{30}$$

where k remains unchanged from the previous case, not corrected by the intermittency.

Planar Jet

In the thin shear layer approximation, the streamwise momentum equation for the planar jet flow is

$$\overline{u}\frac{\partial \overline{u}}{\partial x} + \overline{v}\frac{\partial \overline{u}}{\partial y} = -\frac{\partial}{\partial y}(\overline{u'v'}), \tag{31}$$

and similarly to the wake flow, we can assume that the mean flow is self similar $U = u_0 f(\eta)$. This condition, along with continuity,

$$\frac{\partial \overline{u}}{\partial x} + \frac{\partial \overline{v}}{\partial y} = 0, \tag{32}$$

implies that the lateral velocity is self-similar as well. Casting equations (31) and (32) together and using the self similarity of the mean flow we obtain

$$-\frac{u_0^2}{2\delta}\frac{\partial \delta}{\partial x}\left(f^2 + \frac{f'}{\eta}\int_0^\eta f(\overline{\eta})d\overline{\eta}\right) = -\frac{\partial}{\partial y}\overline{u'v'}. \tag{33}$$

Introducing $f = F'$ and rearranging the equation, we get

$$-\frac{u_0^2}{2\delta}\frac{\partial \delta}{\partial x}\left(F'F\right)' = -\frac{\partial}{\partial y}\overline{u'v'}. \tag{34}$$

Equation (34) is then particularized depending on the closure for the Reynolds shear stresses. Prandtl's mixing length model leads to the following equation,

$$-kF''^2 + FF' = 0, \tag{35}$$

with $k = 2\frac{l_m^2}{\delta^2\delta'}$. This equation has no known analytical solution, hence we solve it numerically. We can again relate the constant k to model constants depending on the type of turbulence cascade:

i) Richardson Kolmogorov cascade:

The mixing length is $l_m = C\delta$, with C constant. The streamwise scalings are $u_0 = AU_{ref}(\frac{x-x_0}{h})^{-1/2}$ and $\delta = Bh(\frac{x-x_0}{h})$, and therefore we get that $k = 2C^2/B$.

ii) Non-equilibrium cascade:

In this case, we have $l_m = C\delta\sqrt{Re_G/Re_{0\delta}}$, and again C is a constant. In this case, the streamwise scalings are $u_0 = AU_{ref}\left(\frac{x-x_0}{h}\right)^{-1/3}$ and $\delta = BL_{ref}\left(\frac{x-x_0}{h}\right)^{2/3}$. Adding the integral form of momentum conservation ($u_0^2\delta = U_{ref}^2 h$), the constant becomes $k = 3\sqrt{\frac{C}{B^3}}$.

Assuming now a constant turbulent eddy viscosity model, the momentum equation particularizes as follows

$$\left(F'^2 + F''F\right) = -kF''', \tag{36}$$

with $k = \frac{2\nu_T}{\delta u_0 \frac{d\delta}{dx}}$. Finally,

$$\left(F'F\right)' = -kF'''. \tag{37}$$

This equation can be solved to obtain the velocity profile $f(\eta) = F'(\eta)$,

$$f(\eta) = sech^2(\eta\sqrt{2k}). \tag{38}$$

Again, depending on the properties of the turbulent cascade, both ν_T and k will adopt different values:

i) Richardson Kolmogorov cascade:

The eddy viscosity takes the form $\nu_T = Cu_0\delta$ with C a constant. Therefore, we get $k = 2CA^2$.

ii) Non-equilibrium cascade:

We have $\nu_T = CU_{ref}L_{ref}$, and the constant becomes $k = 3CA^3$.

Similarly to the axisymmetric wake case, we also study the case of modified eddy viscosity $\nu_T^I = \gamma\nu_T$. Equation (36) then becomes

$$\left(F'F\right)' = -k\gamma F'', \tag{39}$$

whose solution depends on the choice of γ. We propose a function $\gamma = (f(\eta))^m$, relating the intermittency to the mean flow profile. As there is no known closed solution, we numerically solve equation (39).

References

[1] L. Prandtl, Zs. ansgew. Math. Mech **5**, 136 (1925)
[2] A. Townsend, *The structure of turbulent shear flow* (Cambridge University Press, 1976)
[3] W. George, in *Advances in Turbulence*, ed. by W. George, R. Arndt (Springer, 1989)
[4] S. Pope, *Turbulent Flows* (Cambridge University Press, 2000)
[5] P. Chou, Quart. Appl. Math **3** (1945)
[6] S. Goldstein, *Modern developments in fluid dynamics : an account of theory and experiment relating to boundary layers, turbulent motion and wakes* (Clarendon Press, 1938)
[7] A. Townsend, Australian Journal of Chemistry **2**, 451 (1949)
[8] S. Corrsin, NACA Wartime Report **3L23** (1943)
[9] G.Cafiero, J. Vassilicos, Proceedings of the Royal Society A **475**, rspa.2019.0038 (2019)
[10] T. Dairay, M. Obligado, J. Vassilicos, Journal of Fluid Mechanics **781**, 166 (2015)
[11] M. Obligado, T. Dairay, J. Vassilicos, Physical Review Fluids **1**, 044409 (2016)
[12] S. Goto, J. Vassilicos, Physical Review E **94**, 053108 (2016)
[13] J. Vassilicos, Annual Review of Fluid Mechanics **47**, 95 (2015)
[14] M. Lesieur, *Turbulence in fluids: stochastic and numerical modelling* (Nijhoff Boston, MA, 1987)
[15] M. Leschziner, *Statistical turbulence modelling for fluid dynamics-demystified: an introductory text for graduate engineering students* (World Scientific, 2015)
[16] R. Deo, J. Mi, G. Nathan, Experimental Thermal and Fluid Science **32**, 545 (2007)
[17] H. Tennekes, J. Lumley, *A first course in turbulence* (MIT Press, 1972)
[18] P. Johansson, W. George, M. Gourlay, Physics of Fluids **15**, 10.1063/1.1536976 (2003)

[19] A. Kolmogorov, Doklady Akademiia Nauk SSSR **32**
[20] G. Abramovich, *The theory of turbulent Jets* (MIT Press, 1963)
[21] W. Tollmien, Z. angew. Math. Mech pp. 468–478 (1926)